

PAPER • OPEN ACCESS

## Hydrodynamics applied to relativistic heavy ion collisions: influence of equations of state on pion interferometry

To cite this article: D S Lemos *et al* 2015 *J. Phys.: Conf. Ser.* **630** 012032

View the [article online](#) for updates and enhancements.

You may also like

- [A SURVEY OF THE PARAMETER SPACE OF THE COMPRESSIBLE LIQUID DROP MODEL AS APPLIED TO THE NEUTRON STAR INNER CRUST](#)  
W. G. Newton, M. Gearheart and Bao-An Li
- [Single-particle space-momentum angle distribution effect on two-pion HBT correlation in high-energy heavy-ion collisions](#)  
Hang Yang, , Qichun Feng et al.
- [Spectral classification of gravitational-wave emission and equation of state constraints in binary neutron star mergers](#)  
A Bauswein and N Stergioulas



**ECS**  
The  
Electrochemical  
Society  
Advancing solid state &  
electrochemical science & technology

**DISCOVER**  
how sustainability  
intersects with  
electrochemistry & solid  
state science research

# Hydrodynamics applied to relativistic heavy ion collisions: influence of equations of state on pion interferometry

D S Lemos, J Carvalho and O Socolowski Jr

Instituto de Matemática, Estatística e Física, Universidade Federal do Rio Grande, Brazil

E-mail: [denerslemos@gmail.com](mailto:denerslemos@gmail.com)

**Abstract.** In this work we study the effects of a first order phase transition EoS and a lattice QCD based EoS on the pion interferometry. We use a simple hydrodynamical model with cylindrical symmetry and longitudinal boost invariance. We conclude that the results of the HBT radii are very similar for both EoS.

## 1. Introduction

Hydrodynamics has a long history in high-energy collisions [1]. Nowadays, it is an essential tool for describing the collective behaviour of the matter produced in relativistic heavy-ion collisions at RHIC and LHC [2, 3, 4, 5, 6, 7]. Because the hydrodynamical approach involves thermodynamical properties of the system, it is the perfect tool to study the equation of state (EoS) of the strongly interacting matter formed in the collision.

While several hydrodynamical models have successfully used equations of state with first-order phase transition between a hadronic matter and a quark-gluon plasma (QGP), results of lattice QCD have shown that the transition between these phases of matter is not of first-order, but it is of crossover type [8]. It is important to see how the hydrodynamical evolution is affected by the use of different equations of state and how much the observables are affected in these process. Our aim in this work is to perform a study of interferometry of identical pions (HBT effect), by using a simple hydrodynamical model with two different equations of state: an EoS with first-order phase transition between a QGP and a resonance gas with excluded volume correction and a QCD EoS with a crossover transition between the QGP and the hadron phase. The hydrodynamical calculations are performed for central Au + Au collisions at RHIC energy of  $\sqrt{s} = 130A$  GeV, by using cylindrical symmetry and Lorentz boost invariance along the collision axis.

This work is organized as follows. In Sec. 2 we describe the hydrodynamical model used here; in Sec. 3 we show the equations of states used; in Sec. 4 we present the HBT effect; in Sec. 5 we show the numerical results; finally, conclusions are presented in Sec. 6. Much of this work has been presented in [9].

## 2. Hydrodynamic Evolution

In the hydrodynamical description of a relativistic heavy-ion collision, we assume that a matter in local thermal equilibrium is formed and its evolution is governed by the conservation of energy-



momentum and other conserved numbers (baryonic number, strangeness, electric charge, etc.). Here, we assume that all the conserved numbers are zero. Thus, in an arbitrary coordinate system, the hydrodynamic equations are written as [10]

$$T^{\mu\nu}_{;\mu} = \partial_\mu T^{\mu\nu} + \Gamma^\mu_{\sigma\mu} T^{\sigma\nu} + \Gamma^\nu_{\sigma\mu} T^{\mu\sigma} = 0, \quad (1)$$

where  $\Gamma^\mu_{\sigma\nu}$  are the Christoffel symbols. The energy-momentum tensor,  $T^{\mu\nu}$ , for a perfect fluid is given by

$$T^{\mu\nu} = (\varepsilon + P) u^\mu u^\nu - P g^{\mu\nu}, \quad (2)$$

where  $\varepsilon$ ,  $P$ ,  $u^\mu$ , and  $g^{\mu\nu}$  are, respectively, the energy density, the pressure, the fluid flow four-velocity, and the metric tensor. Here, we use a simplified approach for describing the fluid evolution: we suppose transversal and longitudinal expansion by using longitudinal boost invariance [11] and cylindrical symmetry. In this framework, it is more convenient to use hyperbolic-cylindrical coordinates,  $\{\tau, \rho, \phi, \eta\}$ , defined as:  $\tau = (t^2 - z^2)^{1/2}$ ,  $\rho = (x^2 + y^2)^{1/2}$ ,  $\phi = \tan^{-1}(y/x)$ , and  $\eta = (1/2) \ln [(t+z)/(t-z)]$ . The hydrodynamical equations (1) are explicitly written as

$$\partial_\tau T^{\tau\tau} + \partial_\rho [(T^{\tau\tau} + P) v_T] + (T^{\tau\tau} + P) \left( \frac{1}{\tau} + \frac{v_T}{\rho} \right) = 0, \quad (3)$$

$$\partial_\tau T^{\tau\rho} + \partial_\rho (T^{\tau\rho} v_T + P) + T^{\tau\rho} \left( \frac{1}{\tau} + \frac{v_T}{\rho} \right) = 0, \quad (4)$$

where  $T^{\tau\tau} = (\varepsilon + P)\gamma_T^2 - P$  and  $T^{\tau\rho} = (\varepsilon + P)\gamma_T^2 v_T$ , with  $\gamma_T = (1 - v_T^2)^{-1/2}$ . To solve these equations, we need to provide initial conditions and an equation of state.

We assume that the hydrodynamical evolution stops on a sharply defined hypersurface characterized by a freeze-out temperature  $T_{fo}$ . The invariant momentum distribution of observed particles is given by the Cooper-Frye formula [12]

$$E \frac{d^3 N}{dp^3} = \int d\sigma_\mu p^\mu f(x, p), \quad (5)$$

where  $d\sigma_\mu$  is a normal vector to the freeze-out surface and  $f(x, p)$  is the equilibrium distribution function.

### 3. Equation of state

We consider equations of state for a system with zero net baryon density, neutral charge, and neutral strangeness. We compare two types of equations of state: EoS with first order phase transition (1ST), and EoS based on lattice QCD (QCD-s95p).

The EoS 1ST corresponds to a first order phase transition between a hadronic gas, which includes resonances up to 2 GeV and excluded volume correction [13], and a QGP, described by the MIT bag model (see Ref. [2] for details). The critical temperature used in EoS 1ST is  $T_c = 160$  MeV. The EoS QCD-s95p [14] is constructed by using the trace anomaly,  $\Theta^\mu_\mu(T) = \varepsilon(T) - 3P(T)$ , which is evaluated on lattice points. This EoS is parametrized to connect the trace anomaly of a QGP (high temperature) with the trace anomaly of a hadron gas (low temperature). The pressure is calculated by using

$$\frac{P(T)}{T^4} - \frac{P(T_{low})}{T_{low}^4} = \int_{T_{low}}^T \frac{\Theta^\mu_\mu(T')}{T'^5} dT', \quad (6)$$

where  $P(T_{low})$  is the pressure of the hadronic gas. The Fig. 1 shows a comparison of the two EoS.

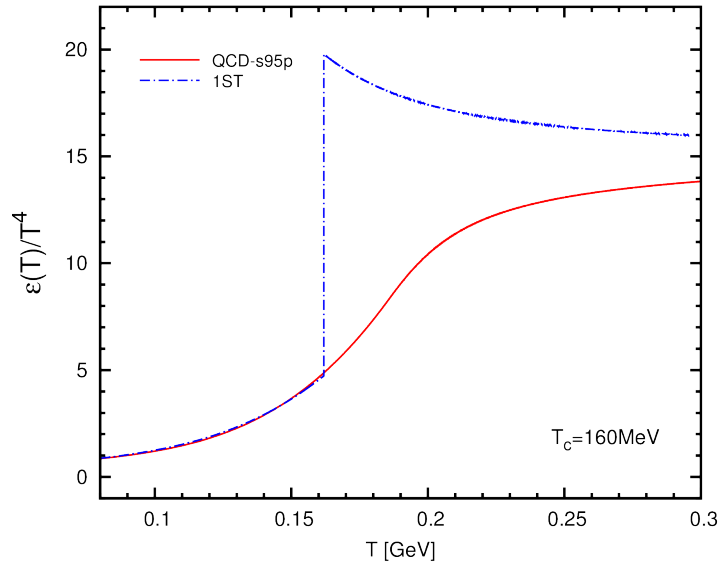


**Figure 1.** Phase diagram comparing the two EoS: first-order phase transition (1ST) and based on lattice QCD (QCD-s95p).

#### 4. Pion interferometry

The interferometry of identical particles (or HBT effect) [15] is a powerful method for probing the space-time geometry of the particle-emitting source. For two particles with four-momenta  $p_1$  and  $p_2$ , we can define the two-particle correlation function as

$$C_2(p_1, p_2) = \frac{\mathcal{P}_2(p_1, p_2)}{\mathcal{P}_1(p_1)\mathcal{P}_1(p_2)}, \quad (7)$$

where  $\mathcal{P}_1$  and  $\mathcal{P}_2$  are, respectively, the one and two-particle inclusive distributions. The two-particle correlation function can be calculated from the emission function,  $S(x, \mathbf{p})$ , which describes the probability of a particle to be emitted from a space-time point  $x$  with momentum  $\mathbf{p}$ . We can write [16, 17]

$$C_2(\mathbf{q}, \mathbf{K}) = 1 + \frac{|\int d^4x \exp(iq \cdot x) S(x, \mathbf{K})|^2}{\int d^4x S(x, \mathbf{K} + \mathbf{q}/2) \int d^4x S(x, \mathbf{K} - \mathbf{q}/2)}, \quad (8)$$

where  $q = p_1 - p_2$  is the relative four-momentum and  $K = (p_1 + p_2)/2$  is the average four-momentum of the pair. The emission function can be written as

$$S(x, \mathbf{p}) = \int d\sigma_\mu(x') p^\mu \delta^{(4)}(x' - x) f(x', \mathbf{p}), \quad (9)$$

where  $f(x, \mathbf{p})$  is the equilibrium distribution function.  $\int d^4x S(x, \mathbf{p})$  coincides with the one-particle spectrum (5).

#### 5. Numerical results

In this section, we show the results for the transverse-momentum distribution and HBT radii for pions calculated by using two equation of state, namely, 1ST and QCD-s95p. To solve the hydrodynamical equations (3) and (4), we use the method RHLLE [21] and simple initial conditions. We consider only central collisions with constant initial energy density of

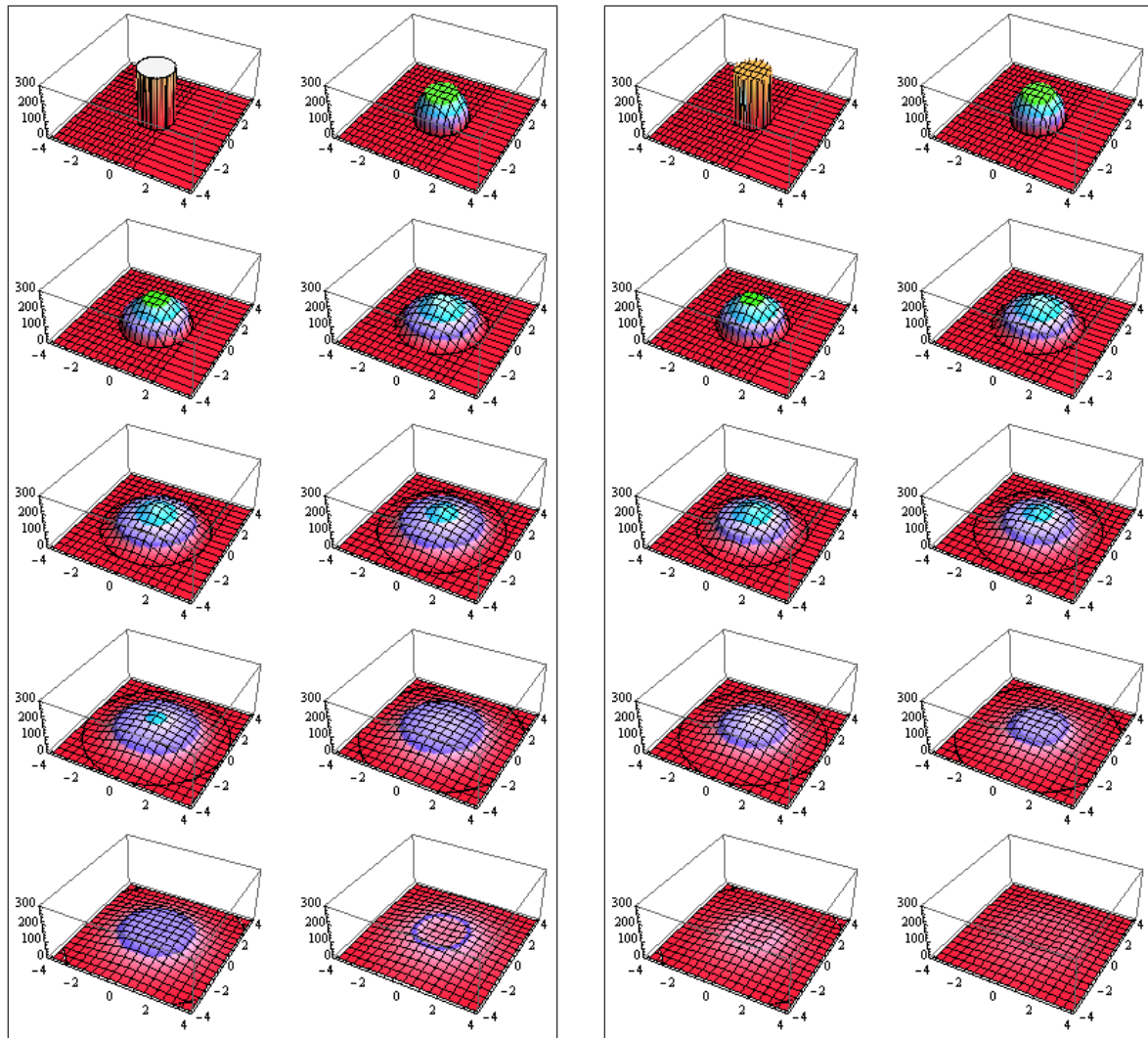


**Figure 2.** Temperature evolution (in MeV) in  $xy$  plane ( $\eta = 0$ ). *Left:* EoS with first-order phase transition is used. *Right:* EoS based on lattice QCD is used. Coordinates  $x$  and  $y$  are in units of the nucleus radius.

$10 \text{ GeV}/\text{fm}^3$ . The initial time is fixed in  $0.3 \text{ fm}$ . We look at two scenarios: (A) without initial transverse velocity; (B) with initial transverse velocity parameterized as [22]  $\tanh(\alpha\rho/R_A)$ , where the parameter  $\alpha = 0.1$  and the nucleus radius  $R_A = 7 \text{ fm}$ .

### 5.1. Transverse-momentum distribution

The transverse-momentum spectra for pions are shown in Fig. 3 for scenario A and in Fig. 4 for scenario B. The figures show the results for the following freeze-out temperatures:  $120 \text{ MeV}$ ,  $130 \text{ MeV}$ ,  $135 \text{ MeV}$ , and  $140 \text{ MeV}$ . We see a small difference between the two equations of state. The  $p_T$  distribution is lightly flatter for QCD-s95p, because, in this equation of state, the pressure is not constant in the crossover transition region causing a larger acceleration of the system. This can be seen in Fig. 2 where the temperature evolution of the fluid is shown for both equations of state: 1ST on the left and QCD-s95p on the right. We see that the fluid cools faster for the QCD-s95p EoS, showing a larger acceleration. We also note that the presence of

an initial transverse velocity (scenario B) gives better results when comparing with experimental data.

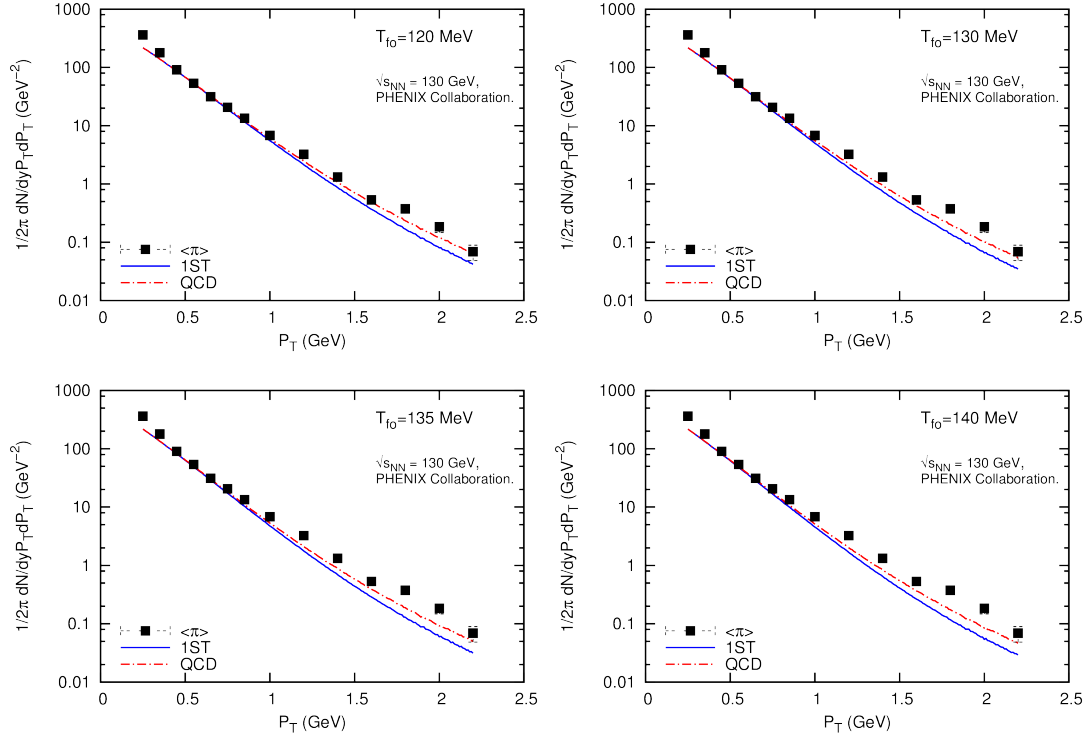


**Figure 3.** Transverse-momentum distributions for pions in Au+Au collisions at 130A GeV, calculated by using four different freeze-out temperatures. Scenario without initial transverse velocity. Comparison of 1ST EoS (solid line) and QCD-s95p EoS (dashed line). Data are from PHENIX collaboration [20]; centrality 0-5%.

### 5.2. HBT radii

We choose the freeze-out temperature  $T_{fo} = 120$  MeV to calculate the HBT radii. To compare our results with experimental data, we use the Bertsch-Pratt *out-long-side* coordinates [16] defined as:

$$q_o = \frac{\mathbf{q}_T \cdot \mathbf{K}_T}{K_T}, \quad q_\ell = q_z, \quad q_s = \frac{(\mathbf{K} \times \mathbf{q})_z}{K_T}, \quad (10)$$

and fit the correlation function (8) with the three-dimensional gaussian

$$C_2(\mathbf{q}, \mathbf{K}) = 1 + \lambda \exp \left[ -R_o^2 q_o^2 - R_\ell^2 q_\ell^2 - R_s^2 q_s^2 \right]. \quad (11)$$

Figures 5 and 6 show the radii  $R_o$ ,  $R_\ell$ ,  $R_s$ , and the ratio  $R_o/R_s$  for the scenarios A and B, respectively, as function of  $K_T$ . The results are compared with experimental data for Au+Au collisions at 130A GeV from PHENIX [19] and STAR [18] collaborations. We can see a small difference between the equations of state, with QCD-s95p EoS giving smaller  $R_o$ ,  $R_\ell$ , and  $R_o/R_s$ . This behaviour is associated with the larger acceleration of the system for QCD-s95p EoS. The  $R_s$  radius does not show any significant difference for the two EoS. It should be noted that the

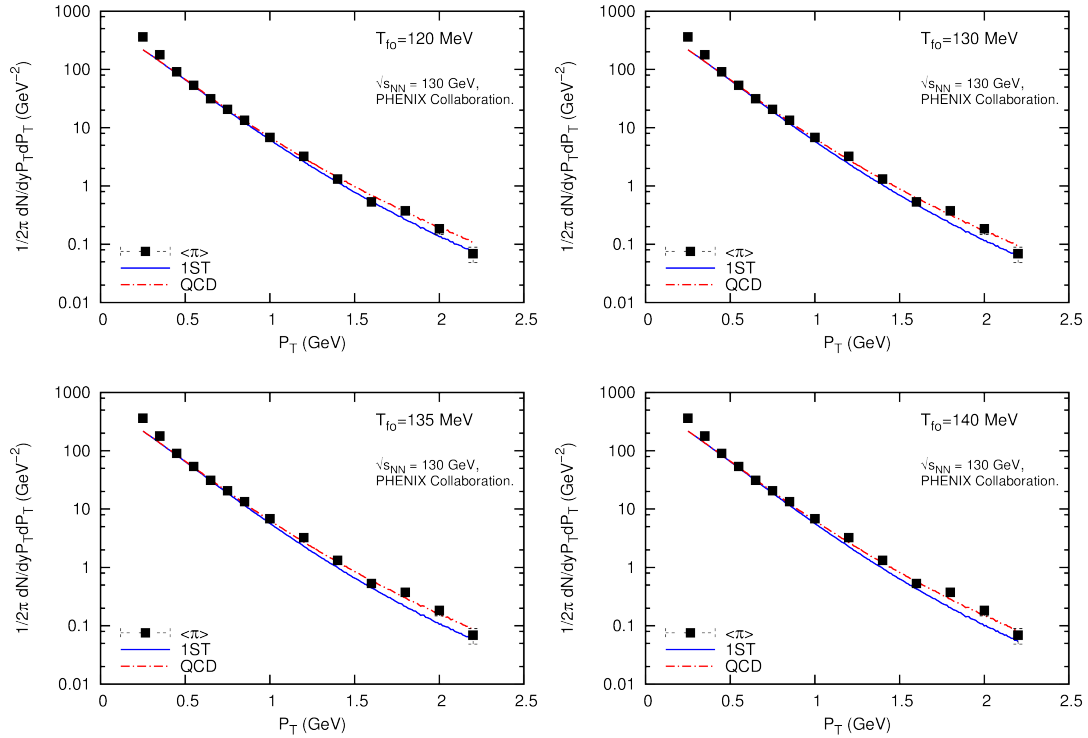


**Figure 4.** Transverse-momentum distributions for pions in Au+Au collisions at 130A GeV, calculated by using four different freeze-out temperatures. Scenario with initial transverse velocity. Comparison of 1ST EoS (solid line) and QCS-s95p EoS (dashed line). Data are from PHENIX collaboration [20]; centrality 0-5%.

scenario B shows a better  $R_o$  and  $R_o/R_s$  behaviour when comparing with experimental data. In scenario A,  $R_o$  radius is approximately constant with  $K_T$ ; in scenario B, it decreases with  $K_T$  (same behaviour shown by experimental data). It shows the importance of initial transverse velocity in explaining the HBT radii, as already discussed in [23].

## 6. Conclusions and Perspectives

In this work, we have used a simple hydrodynamical model in 1+1 dimensions for calculating both  $p_T$  distribution and HBT radii for pions. We have studied the effects of two types of equations of state. We have found that, although the use of different equations of state affects the hydrodynamical evolution, the effects on both  $p_T$  distribution and HBT radii are small. The HBT radii show a tendency to be closer to the data for QCD-s95p EoS, although our numerical results are far from the data.

For a complete understanding of the effects of the equations of state on pion interferometry a more realistic treatment should be done. It includes: hydrodynamics in 3+1 dimensions with viscous effects; event-by-event initial conditions; equations of state with non-zero baryonic chemical potential. Also, others observables should be studied. In part, some of these points are addressed in [24]. In fact, in [25], the HBT effect was studied by using the 3+1 hydrodynamical code NEXSPHERIO, but with a phenomenological parametrization of QCD EoS, that differs from the QCD-s95p EoS used here.

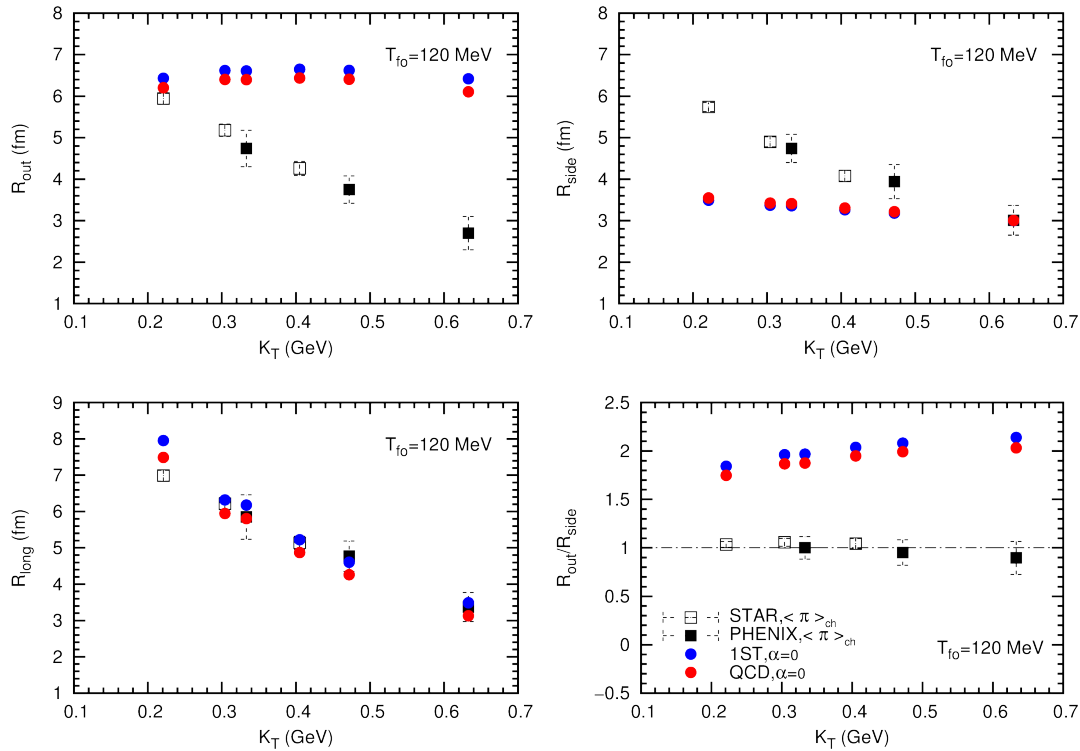


**Figure 5.**  $K_T$  dependence of HBT radii for pions in Au+Au collisions at 130A GeV. Scenario without initial transverse velocity and  $T_{fo} = 120$  MeV. Data are from STAR [18] and PHENIX [19]; most central collisions.

## 7. Acknowledgments

DSL acknowledges the financial support by Universidade Federal do Rio Grande (FURG) for participating in the XXXVII RTFNB.

## References

- [1] Landau L D (1953) *Izv. Akad. Nauk SSSR* **17** 51.
- [2] Hama Y, Kodama T, Socolowski Jr O 2005 *Braz. J. Phys.* **35** 24.
- [3] Socolowski Jr O, Grassi F, Hama Y, Kodama T (2004) *Phys. Rev. Lett.* **93** 182301.
- [4] Andrade R P G, Grassi F, Hama Y, Qian W L (2011) *Nucl. Phys. A* **854** 81.
- [5] Werner K, Karpenko I, Pierog T (2011) *Acta Phys. Polon. Supp.* **4** 629.
- [6] Noronha-Hostler J, Denicol G S, Noronha J, Andrade R P G, Grassi F (2013) *J. Phys. Conf. Ser.* **458** 012018.
- [7] Hirano T (2011) *Acta Phys. Polon. B* **42** 2811.
- [8] Fodor Z, Katz S D (2002) *J. High Energy Phys.* **3** 14; Karsh F (2002) *Nucl. Phys. A* **698** 199.
- [9] Carvalho J 2014 A influência das condições iniciais e das equações de estado no estudo hidrodinâmico da interferometria de píons *Master dissertation* FURG.
- [10] Misner C W, Thorne K S, Wheeler J A (2000) *Gravitation* (Freeman).
- [11] Bjorken J D (1983) *Phys. Rev. D* **27** 140.
- [12] Cooper F, Frye G (1974) *Phys. Rev. D* **10** 186.
- [13] Yen G D, Gorenstein M I, Greiner W, Yang S N (1997) *Phys. Rev. C* **56** 2210.
- [14] Huovinen P, Petreczky P (2010) *Nucl. Phys. A* **837** 26.
- [15] Boal D H, Gelbke C K, Jennings B K 1990 *Rev. Mod. Phys.* **62** 553; Wong C Y (1994) Introduction to High-Energy Heavy-Ion Collisions (World Scientific); Heinz U, Jacak B V 1999 *Ann. Rev. Nucl. Part. Sci.* **49** 529; Florkowski W (2010) Phenomenology of Ultra-Relativistic Heavy-Ion Collisions (World Scientific).

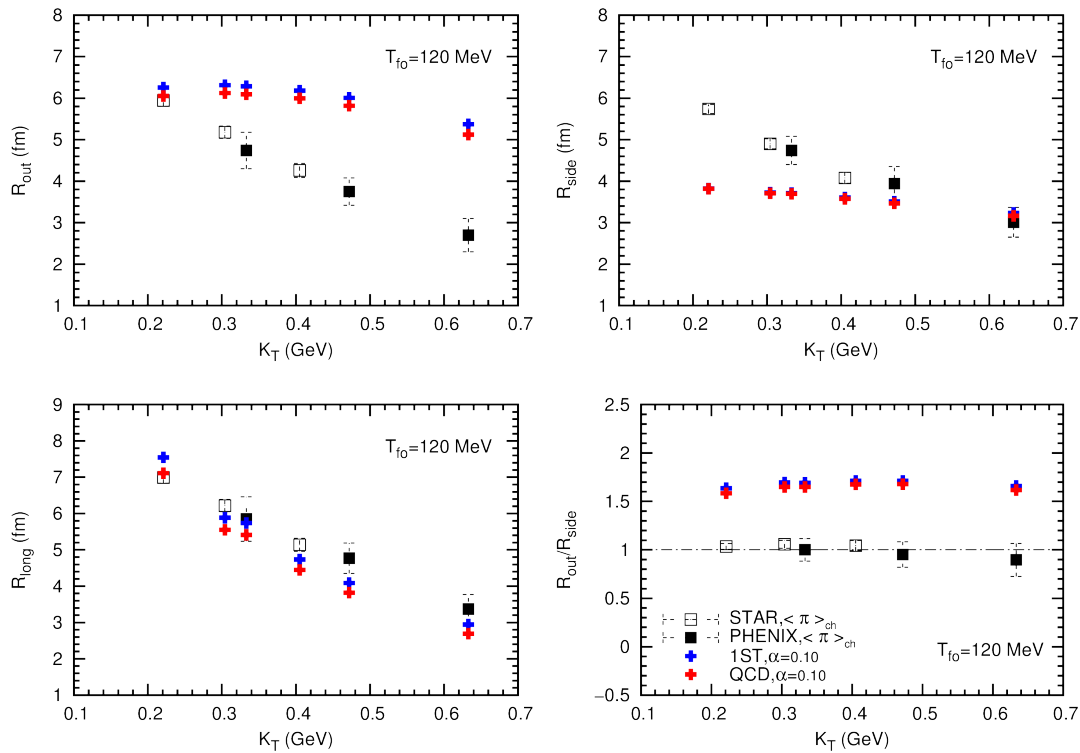


**Figure 6.**  $K_T$  dependence of HBT radii for pions in Au+Au collisions at 130A GeV. Scenario with initial transverse velocity and  $T_{fo} = 120$  MeV. Data are from STAR [18] and PHENIX [19]; most central collisions.

- [16] Lisa M A, Pratt S, Soltz R, Wiedemann U (2005) *Ann. Rev. Nucl. Part. Sci.* **55** 357.
- [17] Wiedemann U A, Heinz U (1997) *Phys. Rev. C* **56** 610.
- [18] Adler C et al (2001) *Phys. Rev. Lett.* **87** 082301.
- [19] Adcox K et al (2002) *Phys. Rev. Lett.* **88** 192302.
- [20] Adcox K et al (2002) *Phys. Rev. Lett.* **88** 242301; Adcox K et al (2004) *Phys. Rev. C* **69** 024904.
- [21] Rischke D H, Bernard S, Maruhn J A (1995) *Nucl. Phys. A* **595** 346.
- [22] Karpenko Iu A, Sinyukov Yu M (2010) *Phys. Rev. C* **81** 054903.
- [23] Pratt S (2009) *Phys. Rev. Lett.* **102** 232301.
- [24] Dudek D M, Qian W L, Wu C, Socolowski Jr O, Padula S S, Krein G, Hama Y, Kodama T. (2014) *Preprint arXiv:1409.0278 [nucl-th]*
- [25] Hama Y, Andrade R P G, Grassi F, Socolowski Jr O, Kodama T, Tavares B, Padula S S 2006 *Nucl. Phys. A* **774** 169